

On the spin distributions of Λ CDM haloes

N. Hiotelis ¹

© Springer-Verlag ●●●●

Abstract We used merger trees realizations, predicted by the extended Press-Schechter theory, in order to study the growth of angular momentum of dark matter haloes. Our results showed that:

- 1) The spin parameter λ' resulting from the above method, is an increasing function of the present day mass of the halo. The mean value of λ' varies from 0.0343 to 0.0484 for haloes with present day masses in the range of $10^9 h^{-1} M_{\odot}$ to $10^{14} h^{-1} M_{\odot}$.
- 2) The distribution of λ' is close to a log-normal, but, as it is already found in the results of N-body simulations, the match is not satisfactory at the tails of the distribution. A new analytical formula that approximates the results much more satisfactorily is presented.
- 3) The distribution of the values of λ' depends only weakly on the redshift.
- 4) The spin parameter of an halo depends on the number of recent major mergers. Specifically the spin parameter is an increasing function of this number.

Keywords galaxies: halos – formation – structure; methods: numerical – analytical; cosmology: dark matter

1 Introduction

There are two more likely pictures regarding the growth of angular momentum in dark matter haloes.

The first is that galactic haloes acquired their angular momentum from the tidal torques of the surrounding matter. This is an old idea of Hoyle (1949) that

has been investigated in a large number of studies (e.g. Peebles 1969; Doroshkevich 1970; Efstathiou & Jones 1979, Barnes & Efstathiou 1987, White 1984; Voglis & Hiotelis 1989, Warren et al. 1992, Steinmetz & Bartelmann 1995). The results of the above studies, analytical and numerical, show that the spin parameter λ , introduced by Peebles (1969) and defined by the relation $\lambda \equiv J\sqrt{|E|}/GM^{5/2}$, has an average value of about 0.05-0.07, where J is the modulus of the spin of halo, M, E are the mass and the energy respectively and G is the gravitational constant. According to the above picture, haloes acquire their angular momentum during their linear stage of their evolution because during this stage they have large linear sizes and thus the environment is capable to affect their evolution by tidal torques. Since their expansion is decelerating their relative linear size becomes smaller and the affection by the environment becomes less significant. The moment of the maximum expansion is in practice the end of the epoch of growth of angular momentum. At latter times, the halo evolves as a dynamically isolated system. Steinmetz & Bartelmann (1995) showed that the dependence of the probability distribution of λ on the density parameter of the model Universe as well as on the variance of the density contrast field is very weak. Only a marginal tendency for λ is found to be larger for late-forming objects in an open Universe.

The second picture is closely related to the hierarchical clustering scenario of cold dark matter (CDM; Blumenthal et al. 1986). According to this scenario, structures in the Universe grow from small initially Gaussian density perturbations that progressively detach from the general expansion, reach a maximum radius and then collapse to form bound objects. Larger haloes are formed hierarchically by mergers between smaller ones, called progenitors. The buildup of angular momentum is a random walk process associated with the mass assembly history of the halo's major progenitor.

N. Hiotelis

1st Experimental Lyceum of Athens, Ipitou 15, Plaka, 10557, Athens, Greece

¹Lysimahias 66, Neos Kosmos, Athens, 11744 Greece, e-mail:hiotelis@ipta.demokritos.gr

The main role of tidal torques in this picture is to produce the random tangential velocities of merging progenitors.

The above two pictures of formation are usually studied by two different kinds of methods. The first kind is the N-body simulations that are able to follow the evolution of a large number of particles under the influence of the mutual gravity, from initial conditions to the present epoch. The second kind consists of semi-analytical methods. Among them, the Press-Schechter (PS) approach and its extensions (EPS) are of great interest since they allow to compute mass functions (Press & Schechter 1974; Bond et al. 1991) to approximate merging histories (Lacey & Cole 1993, Bower 1991, Sheth & Lemson 1999b) and to estimate the spatial clustering of dark matter haloes (Mo & White 1996; Catelan et al. 1998, Sheth & Lemson 1999a).

Recently large cosmological N-body simulations have been performed in order to study the angular momentum of dark matter haloes in Λ CDM models of the Universe (e.g. Bullock 2001, Kasun & Evrard 2005, Bailin & Steinmetz 2005, Avila-Reese et al. 2005, Gottlöber & Turchaninov 2006).

Additionally, semi-analytical methods like merging histories resulting from EPS methods, have been used for similar studies (Vitvitska et. al 2002, Maller et. al 2002).

In this paper, we use such merging histories based on EPS approximations to study the distribution of spins. The paper is organized as follows: In Sect.2, basic equations are summarized. In Sect.3, we present our results while a discussion is given in Sect.4.

2 Construction of merger-trees and acquisition of angular momentum

According to the hierarchical scenarios of structure formation, a region collapses at time t if its overdensity at that time exceeds some threshold. The linear extrapolation of this threshold up to the present time is called a barrier, B . A likely form of this barrier is:

$$B(S, t) = \sqrt{aS_*} [1 + \beta(S/aS_*)^\gamma]. \quad (1)$$

In the above Eq. α , β and γ are constants, $S_* \equiv S_*(t) \equiv \delta_c^2(t)$ where $\delta_c(t)$ is the linear extrapolation up to the present day of the initial overdensity of a spherically symmetric region that collapsed at time t . Additionally, $S \equiv \sigma^2(M)$, where $\sigma^2(M)$ is the present day mass dispersion on comoving scale containing mass M . S depends on the assumed power spectrum. The spherical collapse model has a barrier that does not depend on the mass (eg. Lacey & Cole 1993). For

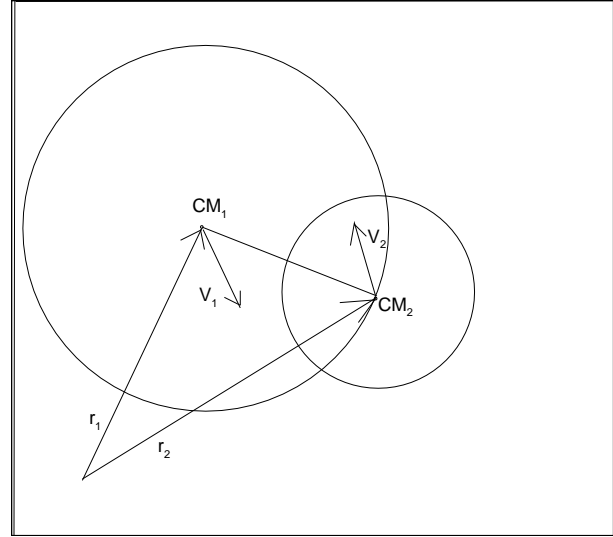


Fig. 1 The figure shows the conditions at the onset of the merger of two haloes with masses m_1 and m_2 and virial radii R_1 and R_2 respectively with $m_1 > m_2$ and $R_1 > R_2$. The centers of their masses are indicated by CM_1 and CM_2 and their distance is $r \equiv \max(R_1, R_2) = R_1$. The position vectors of their centers of mass are \mathbf{r}_1 and \mathbf{r}_2 respectively so their relative position is $\mathbf{CM}_{12} = \mathbf{r}_2 - \mathbf{r}_1$. The vectors of the velocities of their center of mass are \mathbf{v}_1 and \mathbf{v}_2 and the vector of their relative velocity is $\mathbf{v}_{rel} = \mathbf{v}_2 - \mathbf{v}_1$. Haloes merge if they approach each other, that is the condition $\mathbf{v}_{rel} \cdot \mathbf{CM}_{12} < 0$ is fulfilled. See text for more details.

this model, the values of the parameters are $a = 1$ and $\beta = 0$. The ellipsoidal collapse model (EC) (Sheth, Mo & Tormen 2001) has a barrier that depends on the mass (moving barrier). The values of the parameters are $a = 0.707, \beta = 0.485, \gamma = 0.615$ and are adopted either from the dynamics of ellipsoidal collapse or from fits to the results of N-body simulations.

Sheth & Tormen (2002) showed that given a mass element -that is a part of a halo of mass M_0 at time t_0 - the probability that at earlier time t this mass element was a part of a smaller halo with mass M , is given by the equation:

$$f(S, t/S_0, t_0) dS = \frac{1}{\sqrt{2\pi}} \frac{|T(S, t/S_0, t_0)|}{(\Delta S)^{3/2}} \exp \left[-\frac{(\Delta B)^2}{2\Delta S} \right] dS \quad (2)$$

where $\Delta S = S - S_0$ and $\Delta B = B(S, t) - B(S_0, t_0)$ with $S = S(M), S_0 = S(M_0)$.

The function T is given by:

$$T(S, t/S_0, t_0) = B(S, t) - B(S_0, t_0) + \sum_{n=1}^5 \frac{[S_0 - S]^n}{n!} \frac{\partial^n}{\partial S^n} B(S, t). \quad (3)$$

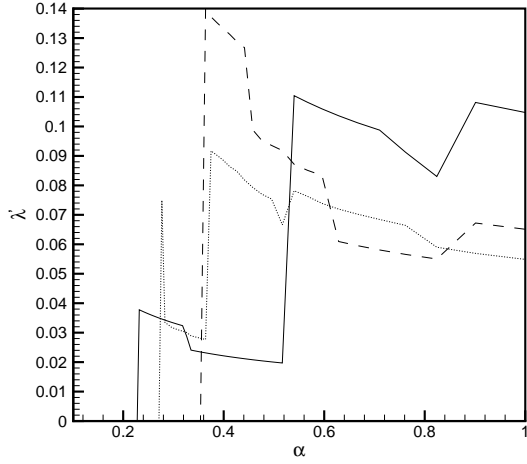


Fig. 2 Spin parameter λ' for the most massive progenitor at scale factor α for the cases 1, 2 and 3. Solid, dashed and dotted lines correspond to the cases 1, 2 and 3 respectively. The evolution of λ' is characterized by sharp increases and decreases due to mergers.

Recently, Zhang & Hui (2006) derived first crossing distributions of random walks with a moving barrier of an arbitrary shape. They showed that this distribution satisfies an integral equation that can be solved by a simple matrix inversion. They compared the predictions of their exact numerical solution with those of approximation given by eq.3 and found a very good agreement. This shows that eq. 3 works well for mildly non linear barriers as that given by eq.1 above.

Eq. 2. can obviously predict the unconditional mass probability, $f(S, t)$, which is simply the probability that a mass element is at time t a part of a halo of mass M , by setting $S_0 = 0$, and $B(S_0, t_0) = 0$. We note that the quantity $Sf(S, t)$ is a function of the variable ν alone, where $\nu \equiv \delta_c(t)/\sigma(M)$. δ_c and σ evolve with time in the same way, thus the quantity $Sf(S, t)$ is independent of time. Setting $2Sf(S, t) = \nu f(\nu)$ one obtains the so-called multiplicity function $f(\nu)$. The multiplicity function is the distribution of first crossings of a barrier $B(\nu)$ (that is why the shape of the barrier influences the form of the multiplicity function), by independent uncorrelated Brownian random walks (Bond et al. 1991). The multiplicity function is related to the comoving number density of haloes of mass M at time t , $N(M, t)$, by the relation,

$$\nu f(\nu) = \frac{M^2}{\rho_b(t)} N(M, t) \frac{d \ln M}{d \ln \nu} \quad (4)$$

that results from the excursion set approach (Bond et al. 1991). In the above Eq., $\rho_b(t)$ is the density of the

model of the Universe at time t .

Using a barrier of the form of Eq.1 in the unconditional mass probability, one finds for $f(\nu)$ the expression:

$$f(\nu) = \sqrt{2a/\pi} [1 + \beta(av^2)^{-\gamma} g(\gamma)] \exp(-0.5av^2 [1 + \beta(av^2)^{-\gamma}]^2) \quad (5)$$

where

$$g(\gamma) = \left| 1 - \gamma + \frac{\gamma(\gamma-1)}{2!} - \dots - \frac{\gamma(\gamma-1) \cdots (\gamma-4)}{5!} \right| \quad (6)$$

Recent comparisons show that the use of EC model improves the agreement between the results of EPS methods and those of N-body simulations. For example, Yahagi et al. (2004) show that the multiplicity function resulting from N-body simulations is far from the predictions of spherical model while it shows an excellent agreement with the results of the EC model. On the other hand, Lin et al. (2003) compared the distribution of formation times of haloes formed in N-body simulations with the formation times of haloes formed in terms of the spherical collapse model of the EPS theory. They found that N-body simulations give smaller formation times (i.e. higher redshifts). Hiotelis & Del Popolo (2006) showed that using the EC model, formation times are shifted to smaller values than those predicted by a spherical collapse model. Additionally, EC model, combined with the 'stable clustering' hypothesis, was used in order to study density profiles of dark matter haloes (Hiotelis 2006). The resulting density profiles at the central regions of haloes have the interesting feature to be closer to the results of observations than the results of N-body simulations. Consequently, the EC model is a significant improvement of the spherical model and therefore we use this model for our calculations.

We assume a number of haloes with the same present day mass M_0 -at present epoch t_0 - and we study their past using merger-trees by finding their progenitors -haloes that merged and formed the present day haloes- at previous times. The procedure for a single halo is as follows: A new time $t < t_0$ is chosen. Then, a value ΔS is chosen from the desired distribution given by Eq.2. The mass M_p of a progenitor is found by solving for M_p the equation $\Delta S = S(M_p) - S(M_0)$. If the mass left to be resolved $M_0 - M_p$ is large enough, the above procedure is repeated so a distribution of the progenitors of the halo is created at t . If the mass left to be resolved -that equals to M_0 minus the sum of the masses of its progenitors- is less than a threshold then, we proceed to the next time analyzing with the same procedure the mass of each progenitor. The most massive progenitor at t is considered as the mass of the initial halo at that

time.

A complete description of the above numerical method is given in Hiotelis & Del Popolo (2006). The algorithm - known as N-branch merger-tree- is based on the pioneered works of Lace & Cole (1993), Somerville & Kollat (1999) and van den Bosch (2002).

In our calculations, we used a flat model for the Universe with present day density parameters $\Omega_{m,0} = 0.3$ and $\Omega_{\Lambda,0} \equiv \Lambda/3H_0^2 = 0.7$. Λ is the cosmological constant and H_0 is the present day value of Hubble's constant. We used the value $H_0 = 100\text{hKMs}^{-1}\text{Mpc}^{-1}$ and a system of units with $m_{unit} = 10^{12}M_{\odot}h^{-1}$, $r_{unit} = 1h^{-1}\text{Mpc}$ and a gravitational constant $G = 1$. At this system of units, $H_0/H_{unit} = 1.5276$.

As regards the power spectrum, we used the ΛCDM form proposed by Smith et al. (1998). The power spectrum is smoothed using the top-hat window function and is normalized for $\sigma_8 \equiv \sigma(R = 8h^{-1}\text{Mpc}) = 1$.

A merger-tree gives the complete history of the halo. After its construction, we know all the progenitors of a halo with present-day, at time $t = t_0$, mass M_0 at a previous time t_1 , all progenitors of every progenitor at t_1 at time $t_2 < t_1$ etc. This procedure is repeated up to a level n of resolution that corresponds to a time t_n . As regards the choice of the time-step we used the procedure described in Hiotelis & Del Popolo 2006 that is: The equation $\delta_c(a_{new}) = \Delta\omega + \delta_c(a_{old})$, where $a_{old} = 1$ at the beginning of the construction, is solved for a_{new} , that is the new value of the scale factor. We used a constant value of $\Delta\omega = 0.1$ but tests with smaller values of $\Delta\omega$ showed no differences in the results. The procedure stops for $a < a_{min} = 0.05$. Then, we start to merge haloes present at time t_n to create the angular momentum history of those haloes that are present to the time level t_{n-1} . We assume that two haloes with virial masses m_1 and m_2 and virial radii r_1 and r_2 merge when the following conditions are fulfilled:

- a) They approach each other.
- b) Their relative energy, given by $E = \frac{1}{2}\mu v^2 - \frac{Gm_1m_2}{r}$, is negative, where $\mu \equiv \frac{m_1m_2}{m_1+m_2}$, r and v are the distance and the relative velocity of their canters of masses.
- c) Their distance r is equal to the the maximum of r_1 and r_2 .

After such a merge a new halo is created with mass $m_{1,2} = m_1 + m_2$ and spin $\mathbf{S}_{1,2}$ given by

$$\mathbf{S}_{1,2} = \mathbf{S}_1 + \mathbf{S}_2 + \mathbf{L}_{\text{orb},1,2} \quad (7)$$

where \mathbf{S}_1 and \mathbf{S}_2 are the spins of the two haloes and $\mathbf{L}_{\text{orb},1,2}$ is their orbital angular momentum given by

$$\mathbf{L}_{\text{orb},1,2} = \frac{m_1m_2}{m_1+m_2}(\mathbf{r} \times \mathbf{v}) \quad (8)$$

\mathbf{r} and \mathbf{v} are the vectors of relative position and velocity of their center of mass respectively. A halo which

has suffered no merger up to a time t has no spin and consequently all haloes at time t_n have no spin. The virial r radius of an halo at scale factor a is related to its virial mass m by the relation:

$$r(a) = \left[\frac{2Gm(a)}{X(a)} \right]^{1/3} \quad (9)$$

where

$$X(a) \equiv \Delta_{vir}(a)\Omega_m(a)H^2(a). \quad (10)$$

$\Omega_m(a)$ and $H(a)$ are the density parameter and the Hubble's constant at scale factor a , respectively. For Δ_{vir} we used the expression given in Bryan & Norman (1998) $\Delta_{vir}(a) \approx (18\pi^2 - 82x - 39x^2)/\Omega_m(a)$ where $x \equiv 1 - \Omega_m(a)$.

The construction of a merger-tree does not requires or predicts any information about the velocity field of merging haloes. Since, in our case, the purpose is to study the growth of angular momentum during a process of subsequent mergers, we need a model for the description of the velocity field. So, at first, we used an arbitrary, but reasonable, model, that is described in details below, satisfying the conditions a) b) and c) set above. Additionally in section 3. we also refer to a model for the velocity field that is consistent with the results of N-body simulations. Both models gave similar results, but the question which model describes the velocity field best is open and under investigation.

The whole procedure of merging the haloes present in the merger-tree model follows:

Let that at level l , a set k haloes with virial masses $m_{l,1}, m_{l,2} \dots m_{l,k}$, virial radii $r_{l,1}, r_{l,2} \dots r_{l,k}$ and spins $\mathbf{S}_{l,1}, \mathbf{S}_{l,2} \dots \mathbf{S}_{l,k}$ consists of all the progenitors of an halo with virial mass $m_{l-1,1}$ and virial radius $r_{l-1,1}$ at level $l-1$. The merger procedure is as follows: Two progenitors $m_{l,1}$ and $m_{l,2}$ merge. First $r = \max(r_{l,1}, r_{l,2})$ and $\mu \equiv \frac{m_{l,1}m_{l,2}}{m_{l,1}+m_{l,2}}$ are calculated. Then, the maximum relative velocity, that satisfies the condition of negative total orbital energy, is found by the relation $v_{max} = (\frac{2Gm_{l,1}m_{l,2}}{r\mu})^{1/2}$. Then, the modulus, v_{rel} , of the relative velocity vector \mathbf{v}_{rel} of the two haloes is picked by a Gaussian distribution with mean value $v_{mean} = v_{max}/2$ and $\sigma = (1/3)v_{mean}$. The two components v_x and v_y are found using uniform distributions in the range $[-v_{rel}, v_{rel}]$. If the condition $v_x^2 + v_y^2 \leq v_{rel}^2$ is satisfied, the third component is found by $v_z = \pm \sqrt{v_{rel}^2 - (v_x^2 + v_y^2)}$, where the sign is chosen randomly. If the above inequality is not satisfied, new values of v_x and v_y are chosen and the procedure is repeated. The components (x, y, z) of the relative position vector \mathbf{r} , with modulus $r \equiv \max(r_{l,1}, r_{l,2})$

are defined choosing x and y by a uniform distribution in the range $[-r, r]$ and then, if the condition $x^2 + y^2 \leq r^2$ is fulfilled, the component z is defined by $z = \pm\sqrt{r^2 - x^2 - y^2}$. The condition of approaching, $\mathbf{r} \cdot \mathbf{v}_{rad} \leq 0$, where \mathbf{v}_{rad} is the radial component of the relative velocity, is checked. If the condition is not fulfilled we go back to choose new velocity components, otherwise we continue by finding the orbital angular momentum, according to (8) and the spin of the newly formed halo according to (7). The mass of this halo is $m_{l,1} + m_{l,2}$, and its virial radius is defined by (9) where a is the scale factor of the Universe at level l . The number of k haloes of the set is now reduced by one. The procedure is repeated until the number of haloes becomes one. Thus, the angular momentum of a new halo, present at time level $l-1$, which had at time level l the above k progenitors, is found. The procedure is repeated for all the sets of progenitors at level l and so the angular momentum for every halo of level $l-1$ is calculated. This new set of haloes consists of the progenitors of haloes at level $l-2$. The same procedure is repeated for level $l-1$ to create the haloes at level $l-2$ and so on. The procedure ends with the formation of a single halo of mass m_0 at level 0 that represents the present age t_0 of the Universe. Fig.1 shows two haloes at the onset of their merger.

As a measure of the angular momentum, we used the parameter λ' given by the (see Bullock et al. 2001; Dekel et al. 2000)

$$\lambda' \equiv \frac{S}{\sqrt{2}mv_c r} \quad (11)$$

where S equals to the spin, m is the virial mass, r the virial radius of the halo and $v_c = \sqrt{Gm/r}$ is the circular velocity at distance r . The parameter λ' is easier to be measured, than λ , not only in simulations but in semi-analytical methods as the merger-tree method used in this paper. This happens because the total energy of the halo is not required. Instead, the calculation of λ requires a known density profile ρ for the halo, the calculation of the potential ϕ by the expression

$$\Phi(r) = -4\pi G \left[\frac{1}{r} \int_0^r \rho(r') r'^2 dr' + \int_r^\infty \rho(r') r' dr' \right], \quad (12)$$

the calculation of the potential energy W

$$W = \frac{1}{2} \int \rho(r) \Phi(r) 4\pi r^2 dr \quad (13)$$

and finally, assuming virial equilibrium, the derivation of the total energy by $E = \frac{1}{2}W$. Simplified forms for specific density profiles can be found in Sheth et. al 2001

It is noticed that the spin parameters λ and λ' are approximately equal for typical Navarro et al. 1997 haloes (Bullock et al. 2001).

3 Results

We studied five cases for haloes of different present day masses m_0 . In our system of units, m_0 takes the values $10^{-2}, 0.1, 1., 10$ and 100 for the cases 1, 2, 3, 4 and 5, respectively. For every case, we produced a number of $N_{res} = 20000 - 60000$ realizations. Studying the progenitors of a halo with present day mass m_0 at some time t_* it is likely to find a number of them with zero angular momenta. This is a consequence of the way of the construction of the merger-tree. These progenitors are haloes that have not suffered any merger for times $t \leq t_*$ and thus either they have not increase their masses at all or they have accreted only small amounts of matter. Notice that the growth of angular momentum resulting by the accretion of amounts of matter that are below a critical value -see Hiotelis & Del Popolo (2006), for the details of the construction of merger trees- is not taken into account in our scheme. The distributions presented below are predicted by taking into account only haloes that have no zero angular momentum.

We note here that the growth of angular momentum in the above presented picture is not so smooth as in the case of the tidal torque theory where the angular momentum is a simple increasing function of time (eg. Barnes & Efstathiou 1987, Voglis & Hiotelis 1989). In the picture studied in this paper, angular momentum increases or decreases in a complicated way. As an example, Fig.2 shows the evolution of λ' as a function of the scale factor a for randomly selected histories from the cases 1, 2 and 3. This picture is characterized by sharp increases and decreases of the spin parameter due to mergers. This is a common behavior present in similar studies (e.g. Vitvitska et. al 2002). In the following we study four important characteristics, of the above picture of the growth of the angular momentum, namely: 1) The form of the distribution of λ' . 2) The dependence of this distribution on the present day mass of the halo. 3) The role of major mergers and their affection on the magnitude and the distribution of λ' , and 4) the dependence of the distribution on the redshift.

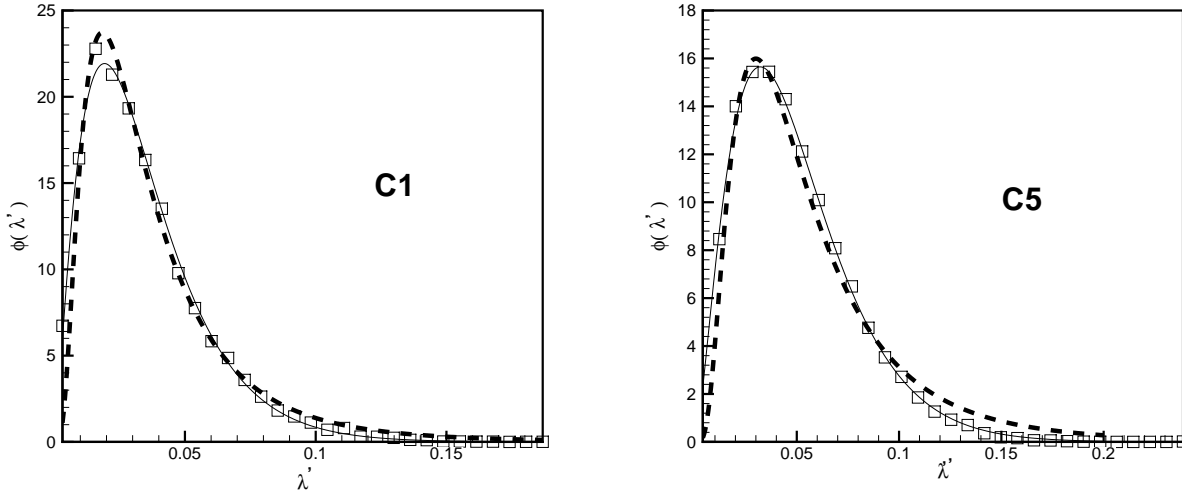


Fig. 3 The present-day, at $z = 0$, distributions of λ' for the cases C1 and C5 are given by squares at the left and the right snapshots, respectively. Dashed lines are the best least-squared fits by a log-normal distribution given in text by eq. 14. Solid lines are also the best least-squared by a distribution given by eq. 15. It is clear that the fits by eq. 15 approximate better the results than the log-normal distribution. In case C5, this is very clear at the right tail of the distribution.

It has been proposed in the literature that the resulting distribution of λ' is well approximated by a log-normal distribution with probability density given by

$$\phi(\lambda') = \frac{1}{\sigma_{\lambda'} \sqrt{2\pi}} \exp \left[-\frac{\ln^2(\lambda'/\bar{\lambda}')}{2\sigma_{\lambda'}^2} \right] \frac{1}{\lambda'}. \quad (14)$$

(e.g. van den Bosch 1998; Gardner 2001; Bailin & Steinmetz 2005). This is a Gaussian in $\ln \lambda'$. The expectation value for $\ln \lambda'$ is $\langle \ln \lambda' \rangle = \ln \bar{\lambda}'$ and it peaks at $\lambda'_{peak} = \bar{\lambda}' \exp(-\sigma_{\lambda'}^2)$. A recent analysis of large cosmological simulation was performed by Bett et al. 2007. These authors used the results of the Millenium simulation of Springel et al. (2005), which followed the evolution of 10 billion dark matter particles in the Λ CDM model, to study the properties of more than 10^6 haloes that were formed. Their study showed that the log-normal distribution cannot approximate well the tails of the resulting distribution so they proposed other alternatives. An alternative of similar form, but rather more general, is used in the present paper. This is of the form:

$$\phi(\lambda') = A \left(\frac{\lambda'}{\lambda'_0} \right)^a \exp \left[-b \left(\frac{\lambda'}{\lambda'_0} \right)^c \right] \quad (15)$$

This distribution peaks at $\lambda'_{peak} = \lambda'_0 \left(\frac{a}{bc} \right)^{\frac{1}{c}}$ and the expectation value for λ' is given by $\langle \lambda' \rangle = \frac{A \lambda'_0^2}{b} \frac{\Gamma(\frac{a+2}{c})}{\Gamma(\frac{a+1}{c})}$ where A, a, b, c, λ'_0 are positive parameters and Γ is the complete gamma function. In Fig.3, we present two

characteristic snapshots for the distributions of λ' , for the cases C1 and C5 that correspond to the smallest and the largest haloes studied. Squares correspond to the results predicted by the method described in this paper, dashed lines correspond to the best least-squared fits of the results by a log-normal distribution while solid lines are the best least-squared fits by a distribution of the form of eq.15. It is clear that distributions given by both eq.14 and eq.15 are good fits of our results for the low mass case C1. For case C5, the log-normal distribution cannot fit well the tails of the solid line. In both cases, the results are described better by eq.15. It is also clear that the distribution depends on the mass of the halo. Although the peaks are located at about the same position in both snapshots, the value of the peak is significantly larger in the case C1. We also note that $\sigma_{\lambda'}$ is a decreasing function of m_0 . It varies from 0.71 for case C1 to 0.67 for case C5. It has also been noticed by other studies (e.g. Vitvitska et al. 2002) that $\langle \lambda' \rangle$ does not depend on the mass of the halo. Fig.3 reveals that this is not true in our results. This can be seen more clearly in Fig.4, where $\langle \lambda' \rangle$ versus the present-day mass of the halo, m_0 , is plotted. Although for a factor of masses 10000 -from 0.01 to 100- $\langle \lambda' \rangle$ varies by a factor only of about 1.41 - from 0.0343 to 0.0484- it is obvious that $\langle \lambda' \rangle$ is an increasing function of mass. Checking the ability of formula (15) to fit the results of Monte-Carlo predictions we found that for $\lambda'_0 = 0.049$ and $c = 1$ we can predict very good fits to all cases, where the values of the rest of the parameters are given in Table 1

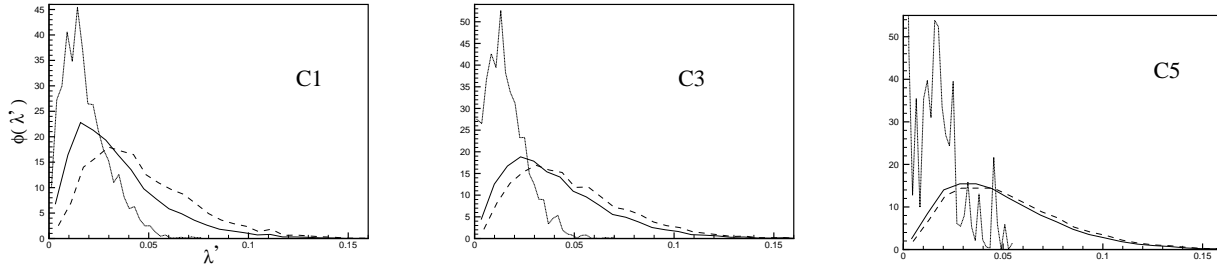


Fig. 5 The role of recent major mergers in the distribution of λ' for the cases C1,C3 and C5. The solid line in every snapshot shows the distribution for all the haloes in every case. Dashed lines show the distribution of the haloes that had at least one recent major merger while dotted lines correspond to the haloes that had no recent major merger.

A and β seem to be decreasing functions of mass. As regards α , this is clearly an increasing function of the mass of the halo.

According to the results of N-body simulations it is likely that spin parameter is a decreasing function of mass. This is supported, for example, by the results of Bett et al. 2007 and Macciò et al. 2007. Additionally, Bett et al. showed that the values of spin parameter and its behavior as a function of mass depends crucially on the halo-finding algorithm. This conclusion was derived by studying three different halo-finding algorithms, the traditional "friends-of-friends" (FOF) algorithm of Davis et al. (1985), the "spherical overdensity" SO of Lacey & Cole (1994) and a new halo definition that they introduced, the TREE haloes. Since the results are so sensitive to the halo-finding algorithm there is a problem regarding the comparison of the results of N-body simulations that have used different halo-finding algorithms. Especially, this problem is more serious for the results that are relative to the growth of angular momentum. In any case, it seems that N-body simulations favor a spin parameter that is a decreasing function of the virial mass. Instead our results as those of Maller et al. (2002) favor the trend that the spin parameter is an increasing function of the virial mass of the halo. Taking into account that our merger-tree algorithm has been constructed independently of that of the above authors, the disagreement with the trend seen in N-body simulations is not likely to arise from inconsistencies in the merger-tree construction al-

gorithm. Additionally the ellipsoidal collapse model we use, that is an improvement of the spherical collapse model used by the above authors, is also incapable to resolve the problem. We also have to note here that a similar trend as that seen in our results is also found, for λ , in the results of Einsele & Loeb (1995) where the collapse of homogeneous ellipsoids in the tidal field of their environment is studied.

In order to study the role of the distribution of velocities we also used a different distribution according to the predictions of N-body simulations of Vitvitska et al 2002 that is defined as follows: Let that haloes with masses M and m and radii R and r merge. For convenience capital letters correspond to the larger halo. After the choice v_{rel} , as described in section 2., we find $v_{cir,M} = (GM/R)^{1/2}$ and $v_{cir,m} = (Gm/r)^{1/2}$. Then the tangential velocity is picked by a Gaussian with mean value $v_{t,mean} = (0.9 - 0.5 \frac{v_{cir,m}}{v_{cir,M}})v_{cir,M}$ for $v_{cir,m}/v_{cir,M} > 0.4$ and $v_{t,mean} = 0.7v_{cir,M}$ for $v_{cir,m}/v_{cir,M} < 0.4$. The above Gaussian has $\sigma = v_{t,mean}/3$. This scheme is consistent to the results of Colin et al. (1999) that major mergers are significantly more radial than minor ones and bring in less specific angular momentum. The differences between the results of this new distribution are those derived by the distribution described in section 2 are negligible and the spin parameter is again an increasing function of the virial mass. However the question remains open.

A number of authors has stressed the role of recent major merger in the final value of the spin parameter. More specifically, they have shown that haloes which have suffered large recent major mergers appear to have larger values of spin parameter. We define as recent mergers those occurred at redshifts $z \leq 3$. We consider the merge between a large halo M and a small m as major if $m/M \geq 0.5$. Obviously a recent major merger satisfies both the above conditions. Figs.5 and 6 show the dependence of the $\langle \lambda' \rangle$ distribution on the number of recent major mergers for three of our

Table 1

Parameters	A	α	β
Case 1	272.206	1.307	3.302
Case 2	222.880	1.292	3.032
Case 3	183.043	1.326	2.76
Case 4	178.417	1.473	2.67
Case 5	187.216	1.719	2.66

cases namely C1, C3 and C5. In Fig.6 solid lines show the distribution of $\langle \lambda' \rangle$ for all haloes of the respective case, while dashed lines are the distributions over those haloes that had at least one recent major merger. Dotted lines are the distributions of haloes that had no recent major mergers. It is clear, particularly at low masses as in case C1, that dashed lines represent distributions that are shifted to the right relative to that represented by solid lines. Thus, haloes that had at least one recent major merger have larger spin parameters. On the other hand, haloes that had no recent major merger -represented by dotted lines- show a narrow distribution shifted to the left, relative to the solid line, that has an obviously smaller mean value.

In Fig. 6 we present $\langle \lambda' \rangle$ for various groups of haloes from the cases C1 and C5 versus the fraction of the total number of haloes of the case that these groups represent. Squares correspond to the case C1, stars to the case C3 and triangles to the case C5. From the left to the right symbols mark the mean value of spin parameter versus the fraction for the following groups: i) all haloes of the case, ii) haloes that had at least one recent major merger, iii) haloes that had at least two recent major mergers and iv) haloes that had at least three recent major mergers. The square inside the circle marks $\langle \lambda' \rangle$ for those haloes of the case C1 that had no recent major mergers. The same is indicated by the star inside the circle and the triangle inside the circle for the cases C3 and C5, respectively. This fig. shows that $\langle \lambda' \rangle$ is an increasing function of the number of recent major mergers. For example, the group, from case C1, of haloes that had at least one recent major merger has $\langle \lambda' \rangle = 0.0461$ and represents 35.6% of the total haloes of the case while the group of haloes that had at least three major merger has $\langle \lambda' \rangle = 0.0545$ and represents only 4% of the total number of haloes of the case. For the group of haloes that had no recent major merger $\langle \lambda' \rangle = 0.0182$, a significantly low value, while the haloes of this group represent 24.3% of the total number of haloes of the case. It is noticed that as the haloes belonging to that last group had an unperturbed recent history, they have time to evolve their gas smoothly to a rotationally supporting disk. Its fraction is an decreasing function of the final halo mass. For case C5 only 0.63% belong to that group. The fraction of haloes with no recent major merger is definitely a decreasing function of the present day mass of the halo. It is quite reasonable, in the hierarchical clustering scenario studied here, that recent major mergers become rare effects for small haloes. It would be interesting to see if, at fixed number of recent major mergers, the distribution of λ' is independent of mass. For this reason, in Fig.7 we plotted the mean value of

λ' for haloes that have suffered the same number of recent major mergers (0,1,2,3 and 4) for all cases. Different symbols correspond to haloes of different masses. Squares correspond to C1, stars to C2, diamonds to C3, circles to C4 and deltas to C5. It is clear from this fig. that for haloes that have suffered the same number of recent major mergers, the heavier one has the larger λ' . Summarizing the results it is yielded that: a) In all cases haloes that had at least one recent major merger have $\langle \lambda' \rangle$ larger than those haloes that had none. b) The fraction of haloes that had at least one recent major merger is larger than the fraction of haloes that had no recent major mergers at all. Thus, we can draw the following conclusions:

- 1) Disk galaxies are found preferentially in small haloes.
- 2) Between haloes of the same mass those that host elliptical galaxies rotate faster than haloes of spiral galaxies (see Vitvitska et al. 2002).
- 3) The number of haloes that had no recent major merges is significantly smaller than the number of haloes that had at least one major merger. If we took into account that major mergers destroy galactic disks and produce spheroidal stellar systems (see, e.g., Barnes 1999) small mergers probably do not (see, e.g., Walker, Mihos & Hernquist 1996) it is natural to expect that haloes which have suffered at least one major merger could not host a spiral galaxy. However spheroidal stellar systems should be more common objects than spiral galaxies.

Fig.8 depicts the dependence of the distribution of spin parameter on the redshift z . Solid lines correspond to present day $z = 0$ while dashed and dotted lines to $z = 1$ and to $z = 3$ respectively. From the left to the right, snapshots correspond to the cases C1, C3 and C5 respectively. Differences between $z = 0$ and $z = 1$ are small. Curves at $z = 1$ appear with smaller peaks and a slight shift, relative to curve for $z = 0$, to the right for small haloes and to the left for larger haloes. Differences between $z = 0$ and $z = 3$ are more obvious. Dashed curves are, for all cases, shifted to the right relative to solid curves. The form of the distributions remains practically unchanged. A shift of the distribution to the right shows that the mean value of the spin parameter becomes larger while a shift to the left shows that it becomes smaller. Thus, the curves indicate that the value of the spin parameter decreases from $z = 3$ to $z = 0$ for all cases. This is verified by the straightforward evaluation of $\langle \lambda' \rangle$ that appears to be systematically smaller at $z = 0$ than its value at $z = 3$.

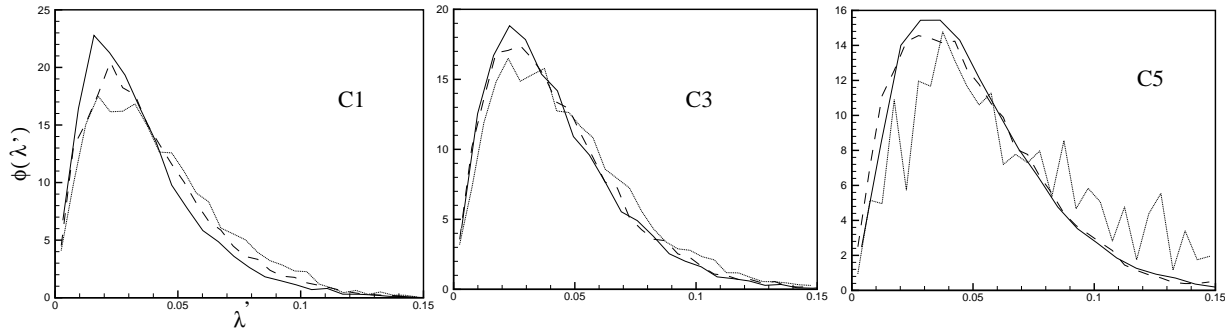


Fig. 8 The dependence of the spin distribution on the redshift z . Solid lines correspond to present day, $z = 0$ while dashed and dotted lines correspond to $z = 1$ and to $z = 3$. From the left to the right, snapshots correspond to the cases C1, C3 and C5, respectively. It is shown that the distribution of λ' is, to a good approximation, unchanged between $z = 0$ and $z = 1$. Differences between $z = 0$ and $z = 3$ are more obvious but without a significant change of the shape of the distribution.

4 Discussion

This study describes a picture for the growth of the angular momentum of dark matter haloes in terms of a hierarchical clustering scenario. The results presented above are, in general, in good agreement with the results that were already known in the literature. Comparing our results with those of large N-body simulations, we have found satisfactory agreement in the following points:

- 1) The values of spin parameter are in the range of 0.0343 to 0.0484 for haloes with present day masses in the range of $10^9 h^{-1} M_\odot$ to $10^{14} h^{-1} M_\odot$.
- 2) A log-normal distribution approximates satisfactorily the distributions of the values of the spin parameter but it fails to describe accurately the tails of the resulting distributions. A new, more satisfactory formula, is presented.
- 3) The role of recent major mergers is very important. The distribution of the spin parameter is appreciably affected by the number of recent major merger. The present day value of the spin parameter of a halo is an increasing function of the number of the recent major mergers.
- 4) The distributions of the spin parameter do not depend significantly on the redshift.
- 5) The value of the spin parameter is a function of the present day mass of the halo. The form of this function depends, in N-body simulations, on the halo-finding algorithm but in general seems that spin parameter is a decreasing function of mass. Instead, in our results, $\langle \lambda' \rangle$ is an increasing function of mass, approximately very closely a power-law form.

Our results give rise to some questions, as for example: Why semi-analytical methods are not able to predict the correct relation between the spin parameter and the

virial mass of the halo? Does this disagreement reflects the null role of tidal fields in the orbital-merger picture or it arises from other problems associated with the nature of merger-trees? Are merger-trees able to give the correct relation for better description of the velocity field during the merge? Is any way improvements on both analytical and numerical methods are required in order to help us answering some of the above questions and to advance our understanding about the physical processes that created the structures we observe.

5 Acknowledgements

We acknowledge the anonymous referee for useful comments and suggestions, Dr. M. Vlachogiannis and K. Konte for assistance in manuscript preparation, and the *Empirikion* Foundation for its financial support.

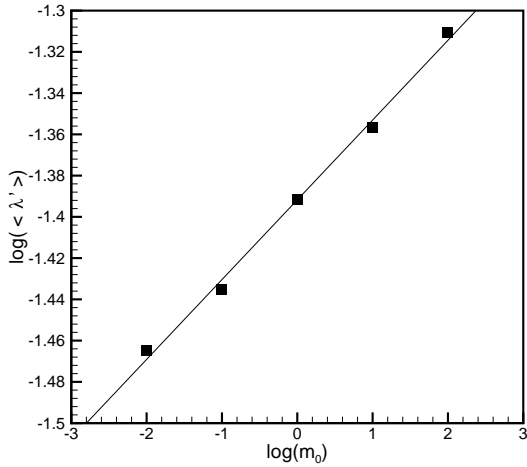


Fig. 4 The mean value of λ' as a function of the present day mass m_0 of the halo. Although the values of λ' are not very sensitive to the values of the mass, as they vary from 0.0343 to 0.0489 for a range of mass 0.01 to 100, our results show that $\langle \lambda' \rangle$ is an increasing function of the mass of the halo. The linear dependence shown, $\log(\langle \lambda' \rangle) \approx -1.392 + 0.0387 \log(m_0)$, in this figure indicates that $\langle \lambda' \rangle$ varies as a power of m_0 .

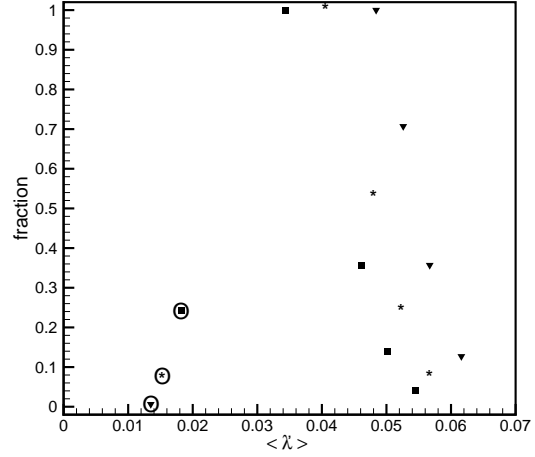


Fig. 6 The role of recent major mergers for the cases C1,C3 and C5. The horizontal axis shows values of $\langle \lambda' \rangle$ while the vertical one represent the fractions of various groups of haloes. Squares correspond to the case C1, stars to the case C3 and triangles to the case C5. From top to bottom symbols mark the mean value of spin parameter versus the fraction for the following groups: i) all haloes of the case, ii) haloes that had at least one recent major merger, iii) haloes that had at least two recent major mergers and iii), haloes that had at least three recent major mergers. The square in the circle marks $\langle \lambda' \rangle$ for those haloes of the case C1 that had no recent major mergers. The same hold for the star inside the circle and the triangle inside the circle but for the cases C3 and C5 respectively. See text for more details.

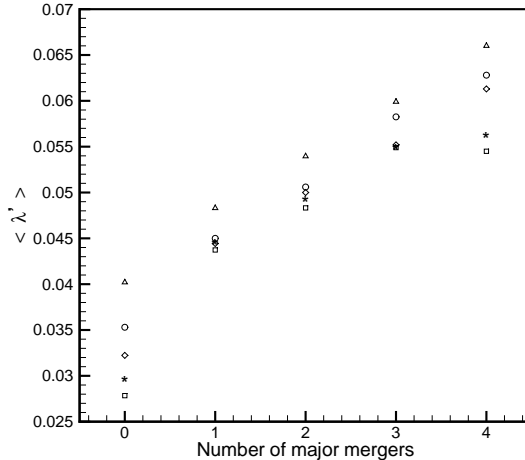


Fig. 7 This figure presents the distribution of spin parameter at fixed number of recent major mergers (0,1,2,3 and 4). Different symbols correspond to haloes of different masses. Squares correspond to C1, stars to C2, diamonds to C3, circles to C4 and deltas to C5. It is clear that even at fixed number of recent major mergers the distribution of λ' is an increasing function of the mass of the halo.

References

- Avila-Reese V., Colín P., Gottlöber S., Firmani C., Maulbetsch C., 2005, *ApJ*, 634, 51
- Bailin J., Steinmetz M., 2005, *ApJ*, 627, 647
- Barnes J.E., Efstathiou G., 1987, *ApJ*, 319, 575
- Barnes J.E., 1999 in *ASP Conf. Ser.* 187, *The Evolution of Galaxies on Cosmological Timescales*, ed. J.E. Beckman & T.J. Mahoney (San Francisco:ASP), 293
- Bett, P., Eke, V., Frenk, C.S., Jenkins, A., Helly, J., Navarro, J., astro-ph/0608607v3
- Blumenthal G.R., Faber S.M., Flores R., Primack J.R., 1986, *ApJ*, 301, 27
- Bond, J.R., Cole S., Efstathiou G., Kaiser N., 1991, *ApJ*, 379, 440
- Bower, R., 1991, *MNRAS*, 248, 332
- Bryan G., Norman M., 1998, *ApJ*, 495, 80
- Bullock, J. S., Kolatt, T. S., Sigad, Y., Somerville, R. S., Kravtsov, A.V., Klypin, A. A., Primack, J. R., Dekel, A., 2001, *MNRAS*, 321, 559
- Catelan, P., Lucchin F. Matarrese, S., Porciani, C., 1998, *MNRAS*, 297, 692
- Colín, P., Klypin, A.A., Kravtsov, A.V., 2000, *ApJ*, 539, 561
- Davis M., Efstathiou G., Frenk C.S., White S.D.M., 1985, *ApJ*, 292, 371
- Dekel A., Bullock J.S., Porciani C., Kravtsov A.V., Kollat T.S., Klypin A.A., Primack J.R., 2000, in *Funes J.G.S.J., Corsini E., eds ASP conf. Ser. Vol. 230, Galaxy Disks and Disk Galaxies*. Astron. Soc. Pac., San Francisco, p.565
- Doroshkevich A.G., 1970, *Astrofizika*, 6, 581
- Efstathiou G., Jones B.J.T., 1979, *MNRAS*, 186, 133
- Eisenstein D.J., Loeb A., 1995, *ApJ*, 439, 520
- Gardner J.P., 2001, *ApJ*, 557, 616
- Gottlöber S., Turchaninov V., 2006, astro-ph/0511675
- Hiotelis N., Del Popolo A., 2006, *ASS*, 301, 167
- Hiotelis N., 2006, *A&A*, 458, 31
- Hoyle F., 1949, in *Burgers J.M., van de Hulst H.C., eds, Problems of Cosmical Aerodynamics, The Origin of the rotations of the galaxies*, Central Air Documents Office, Dayton, OH, pp195-197
- Kasun S.F., Evrard A.E., 2005, *ApJ*, 629, 781
- Lacey, C., Cole, S., 1993, *MNRAS*, 262, 627
- Lacey, C., Cole, S., 1994, *MNRAS*, 271, 676
- Lin W.P., Jing Y.P., Lin L., 2003, *MNRAS*, 344, 1327
- Macciò A.V., Dutton A.A., van den Bosch F.C., Moore B., Potter D., Stadel J., *MNRAS*, 2007, 378, 55
- Maller, A.H., Dekel, A., Somerville, R., *MNRAS*, 2002, 329, 423
- Mo, H.J., White, S.D.M., 1996, *MNRAS*, 282, 347
- Navarro, J.F., Frenk, C.S., White, S.D.M., 1997, *ApJ*, 490, 493
- Peebles P.J.E., 1969, *ApJ*, 155, 393
- Press, W., Schechter, P., 1974, *ApJ*, 187, 425
- Sheth, R.K., Lemson, G., 1999a, *MNRAS*, 304, 767
- Sheth, R.K., Lemson, G., 1999b, *MNRAS*, 305, 946
- Sheth, R.K., Hui, L., Diaferio, A., Scoccamarro, R., 2001, *MNRAS*, 325, 1288
- Sheth, R.K., Tormen G., 2002, *MNRAS*, 329, 61
- Smith, C.C., Klypin, A., Gross, M.A.K., Primack, J.R., Holtzman, J., 1998, *MNRAS*, 297, 910
- Somerville, R.S., Kollat, T.S., 1999, *MNRAS*, 305, 1
- Springel et al., 2005, *Nature*, 435, 629
- Steinmetz M., Bartelmann M., 1995, *MNRAS*, 272, 570
- Yahagi, H., Nagashima, M., Yoshii, Y., 2004, *ApJ*, 605, 709
- van den Bosch, F.C., 1998, *ApJ*, 507, 601
- van den Bosch, F.C., 2002, *MNRAS*, 331, 98
- Vitvitska V., Klypin A.A., Kravtsov, A.V., Wechsler, R.H., Primack, J.R., Bullock, J.S., *MNRAS*, 2002, 581, 799
- Voglis N., Hiotelis N., *A&A*, 1989, 218, 1
- Walker I.R., Mihos J.C., & Hernquist L. 1996, *ApJ*, 460, 121
- Warren M.S., Quinn P.J., Salmon J.K., Zurek W.H., 1992, *ApJ*, 399, 405
- White S.D.M., 1984, *ApJ*, 379, 52
- Zhang J., Hui L., 2006, *ApJ*, 641, 641